Scaling of Hydrologic Conceptualisations: Approaches to Handling Subgrid Variability

N.R. Viney[a] and M. Sivapalan[b]

[a] CSIRO Land and Water, Private Bag No. 5, Wembley, WA 6913, Australia (Neil.Viney@csiro.au)

[b] Centre for Water Research, Department of Environmental Engineering, University of Western Australia, 35 Stirling Highway, Crawley, WA 6009, Australia

Abstract: A fundamental question in scale research is how to scale up descriptions of hydrological responses from the small scales at which they are developed to larger scales at which predictions are required or can be validated, in the presence of both spatial heterogeneity of soils, vegetation and topography, and space-time variability of climatic inputs. One scaling approach is the disaggregation-aggregation approach, which involves disaggregating catchment-scale state variables to point-scale distributions, applying a suitable point-scale physical model using these state variables, and aggregating the resulting point-scale responses to yield a catchment-scale response. Thus, the approach provides a way of linking the catchment-scale state variables with the catchment-scale responses and thereby permits the development of empirical large-scale models that still retain some essence of the small-scale physics. In this paper we illustrate the disaggregation-aggregation approach with two examples that deal with developing catchment-scale conceptualisations of (a) infiltration excess runoff and (b) evapotranspiration, using detailed process-based models available at the small scale. These conceptualisations became the building blocks of the large-scale catchment model, LASCAM.

Keywords: Scaling up; Aggregation; Disaggregation; Model conceptualisations; Subgrid variability

1. INTRODUCTION

Large-scale conceptualisations of hydrological processes are needed for the development of catchment-scale rainfall-runoff models, and subsequently water quality models, and also for linking surface hydrology to global climate models. Ideally, these models should implicitly account for sub-grid variability in the hydrological responses. Although point-scale hydrological processes are well understood and readily represented in physically-based models, it is now well recognised that for most hydrological processes, the use of effective parameters, let alone average parameters, is not appropriate due to the strong nonlinearity of the process descriptions. In the past, hydrologists have usually resorted to conceptual models, often based on functions chosen arbitrarily, and whose parameters must be estimated by calibration. Because these parameters are estimated without reference to process-based descriptions, the conceptual models are not physically-based in that knowledge of the small-scale landscape properties (e.g., soil hydraulic properties) cannot be used to estimate, or in any way be related to, these parameters.

Let us denote the small-scale hydrological responses by $f(s, \theta, I)$ and the corresponding larger-scale responses by $F(S, \Theta, I)$, where s and S denote state variables (e.g., soil moisture), i and I represent climatic inputs (rainfall, potential evaporation) and θ and Θ are vectors representing landscape properties (i.e., parameters). In general, s and i may vary in both space and time, while θ varies in space only. If the function f is linear then the scaling up problem is trivial since f will remain invariant, and model parameters at the larger scale can be estimated by some kind of averaging of the small-scale values.

The problem in large-scale hydrological modelling is to obtain some representation of the large-scale response, F, in terms of the large-scale variables, (S, Θ, I). There is therefore a real need to estimate not only the larger scale parameter values but also to derive the corresponding, as yet unknown, functional forms ($f \rightarrow F$), along with the scaling connections between the state variables ($s \leftrightarrow S$) and parameter values ($\theta \leftrightarrow \Theta$).

To overcome some of these shortcomings, Sivapalan [1993] proposed a modelling framework based on a disaggregation-aggregation approach that implicitly incorporates knowledge of point scale processes into large scale conceptualisations. The approach involves three stages (Figure 1). Firstly, disaggregation operators are developed to scale the state variables from large to point scale ($S \rightarrow s$). Secondly, we use the known point-scale physics, together with known point-scale parameters, θ, to evaluate f at each point in the domain. Finally, we aggregate the point scale responses across the catchment to derive

a catchment scale response, F. This approach now gives us a way of connecting S with F (the dashed line in Figure 1). We can therefore investigate the functional dependence of F on S, and develop empirical relationships describing this dependence. Furthermore, we can also use this approach to infer relationships between θ and Θ. The two examples presented in this paper assume that the climatic inputs are constant in space, but clearly the modelling approach can be extended by incorporating downscaling schemes for the climatic variables.

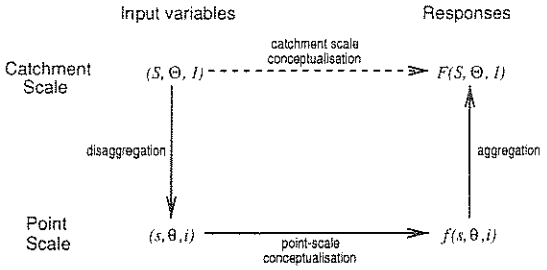

Figure 1. Functional relationships between input variables and responses at large and small scales.

Sivapalan [1993] addressed only the first of the stages described above. He developed steady state scaling relationships between S and s that are conditioned on topography, climate and vegetation cover. We use these relationships here in the first example: predicting catchment scale infiltration capacities and infiltration-excess runoff in terms of catchment scale storages. The second example involves the development of equations for predicting and partitioning evaporation among three conceptual stores.

2. INFILTRATION-EXCESS RUNOFF

Although great strides have been made in the modelling of infiltration and runoff generation in the past four decades, even the best existing solutions for the infiltration problem have only been obtained for one-dimensional infiltration and for the simplest of boundary and initial conditions. Unfortunately, these solutions do not translate well to the real world, where moisture content is variable in space and time and the boundary conditions are quite complex and variable. To date, too little research has been carried out on investigating the linkages between the micro-scale, process-based descriptions of infiltration and possible macro-scale conceptualisations. In this section we describe a methodology for deriving lumped, physically-based parameterisations of infiltration and runoff generation in heterogeneous catchments.

At any point on the surface of the catchment, the local infiltration capacity and infiltration rate are modelled using an extension of the Green and Ampt [1911] equation, modified to allow for a non-uniform initial moisture content in equilibrium with a water table at finite depth and the exponential decrease of saturated hydraulic conductivity with depth. The catchment is subjected to a number of simulated rain storms of varying intensity and duration. By applying the point infiltration model for all points on the catchment, catchment averages of infiltration capacity, infiltration rate and cumulative infiltration volume are computed for these storm events. Based on this simulation approach, empirical relationships are established between the catchment-scale infiltration capacity and the corresponding catchment-scale cumulative infiltration volume for different antecedent conditions.

The exponential decrease of the saturated hydraulic conductivity with with depth z from the ground surface is given by

$$K_s(z) = K_s(0)\exp(-fz)$$

where $K_s(0)$ is the surface value and f is a decay parameter. We assume that all other soil hydraulic properties remain constant with depth. Hydraulic conductivity, K, suction head, ψ, and moisture content, θ, are assumed to follow the characteristic relations proposed by Brooks and Corey [1964].

To describe the spatial variability of antecedent soil moisture, we use the TOPMODEL formulation of Beven and Kirkby [1979], as modified by Sivapalan et al. [1990]. This model is based upon the fundamental assumption that, under quasi-steady conditions, the difference between the local pre-storm water table depth D_i and its catchment-wide average, $\overline{D}$, is linearly related to the corresponding difference between the topography-soil index, $\ln[aT_e/(T_i \tan\beta)]$, and its catchment average, λ. This relationship can be expressed by

$$D_i = \overline{D} - \frac{1}{f}\left(\ln\left(\frac{a_i T_e}{T_i \tan\beta}\right) - \lambda\right) \qquad (1)$$

where a_i is the area draining through location i per unit contour length, T_i is a local transmissivity, $\tan\beta$ is the local slope and T_e is an effective catchment mean of T_i. Given $\overline{D}$ and the spatial pattern of values of the topography-soil index, (1) enables the prediction of the local initial water table depth D_i for all points within the catchment. Thus, as Sivapalan [1993] pointed out, (1) represents the linkage between the state variables representing the permanent groundwater table system at the local and catchment scales.

Prior to the storm, those parts of the catchment that are saturated are those where the value of the topography-soil index is such that the local depth to groundwater is less than the thickness of the capillary fringe, ψ_c. These regions expand and contract both during storms and seasonally, and their areal extent and locations can also be predicted by the model. If it can be assumed that the water table depth, D_i, and the soil moisture deficit, S_i, are uniquely related by a function $D_i = h(S_i)$, then surface saturation will occur at those points where the volume of infiltrated water at any given time, $G_i(t)$,

exceeds the local initial soil moisture deficit. This condition may be expressed by

$$\ln\left(\frac{a_i T_e}{T_i \tan\beta}\right) \geq \lambda + f\left(\overline{D} - h\left(G_i(t)\right)\right) \qquad (2)$$

Now, using the Brooks and Corey relationships and (2), the total volumetric moisture deficit in the vertical soil profile may be obtained by integrating $\theta_s - \theta_i(z)$ between the ground surface ($z = 0$) and the top of the capillary fringe ($z = D_i - \psi_c$) to yield

$$S_i(D_i) = (\theta_s - \theta_r)\left(D_i - \psi_c - \frac{1}{(1-\delta)}\left(\left(\frac{\psi_c}{D_i}\right)^{\delta} D_i - \psi_c\right)\right) \qquad (3)$$

if $D_i > \psi_c$, with $S_i(D_i) = 0$ otherwise. Here, θ_s is the saturation moisture content, θ_r is the residual moisture content and δ is a parameter in the Brooks and Corey model. The total moisture deficit in the entire catchment, S_B, can be expressed in terms of the average water table depth $\overline{D}$ by integrating S_i over all possible values of the topography-soil index.

Following the traditional Green and Ampt formulation, we assume the existence of a sharp, rectangular wetting front. The volume of infiltrated water $G_i(t)$ when the wetting front has reached an average depth of L_f is given by

$$G_i(L_f) = S_i(D_i) - S_i(D_i - L_f) \quad \text{for } L_f < D_i - \psi_c$$

This equation may be inverted numerically to give the depth to the wetting front, $L_f(G_i)$ as a function of the cumulative infiltration volume, G_i. The infiltration capacity of the soil at any point on the ground surface, g^*, when the wetting front is at depth L_f is then given by

$$g_i^* = g_i^*(G_i) = \frac{L_f(G_i)\left(1 + \psi_0\left(L_f(G_i)\right)/L_f(G_i)\right)}{\int_0^{L_f(G_i)} K_s^{-1}(z)\,dz} \qquad (4)$$

where ψ_0, the suction at the wetting front, can be expressed in terms of the soil moisture characteristics. The fact that ψ_0 is independent of K_s means that (4) can be used to estimate g^* for any type of variation of K_s with depth. For the special case where K_s decreases exponentially with depth, (4) becomes

$$g_i^*(G_i) = \frac{K_s(0) f L_f(G_i)}{\exp\left(f L_f(G_i)\right) - 1}\left(1 + \psi_0\left(L_f(G_i)\right)/L_f(G_i)\right)$$

Knowing $g_i^*(G_i)$, the actual infiltration rate, $g_i(t)$, at any time, t, during a rainfall event is calculated as the lesser of g_i^* and the local, instantaneous rainfall intensity, $p_i(t)$. The rate of infiltration-excess runoff is then given by $q_i(t) = p_i(t) - g_i(t)$. Clearly, to scale these instantaneous, point predictions of $g_i(t)$ and $q_i(t)$ up to the scale of a catchment and the duration of an event, we must integrate them over space and time.

The runoff prediction model is applied to two small, adjacent catchments in southwestern Western Australia, Wights (0.94 km^2) and Salmon (0.82 km^2). Due to the very high permeabilities of the gravelly surface soils of these catchments, almost all the rainfall reaching the ground infiltrates and rapidly percolates down to the level of the less permeable clayey layer at 2–5 m depth. Subsurface runoff generated at this interface then flows downslope and contributes to the formation of a perched groundwater table. The volume of this subsurface infiltration-excess runoff is affected by the antecedent soil moisture at the surface of the clay horizon, which in turn is influenced by the local depth to the permanent groundwater table.

For the two catchments, the distributions of the topographic index are derived from digital elevation maps and used with (1) to disaggregate an assumed mean water table depth to determine the local water table depths, D_i, at every point in the catchment. The local soil moisture deficits are then calculated using (3), which, on integration, yields the catchment-scale soil moisture deficit, S_B. The initial contributing area is given by (2) and indicates those parts of the catchment on which all rainfall immediately runs off. As the storm progresses, this area expands as water infiltrates the unsaturated locations and begins to fill the soil moisture deficit.

This model was used to simulate infiltration and runoff generation on the two catchments under a variety of conditions involving different combinations of the soil hydraulic properties ($\overline{K_s(0)}$ and f) and antecedent wetness ($\overline{D}$), and with storms of varying depth, duration and frequency.

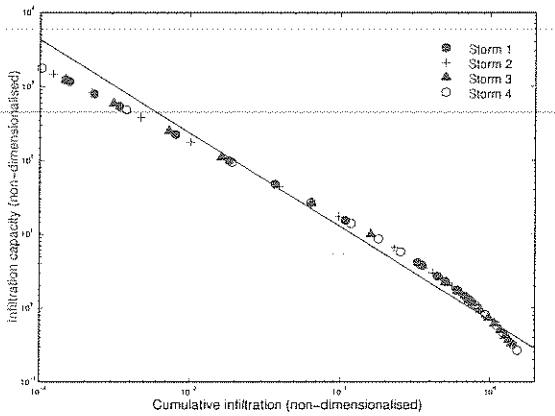

Figure 2. The relationship between $\overline{g^*}$ and $\overline{G}$ for four storms of varying intensity and duration. The solid line depicts the linear regression of the data points.

The variations of $\overline{g^*}$ with $\overline{G}$ for a variety of storms, but with all other parameters kept constant (Figure 2) clearly support the adoption of a unique $\overline{g^*}$ versus $\overline{G}$ relationship. The straight lines of the log-log graph in Figure 2 suggest a relationship of the form

$$\overline{g^*} = a\overline{G}^{-b}$$

where a and b are regression constants that are likely to depend on the catchment attributes, $\overline{D}$, f and $\overline{K_s(0)}$.

To test this dependence, a series of simulations was performed by varying $\overline{D}$ while keeping the other parameters constant. The results (Figure 3) show a set of almost parallel lines on a log-log graph, thus suggesting that the slope parameter, b, is independent of $\overline{D}$, but that the intercept parameter, a can be postulated as a function of $\overline{D}$ (or S_B).

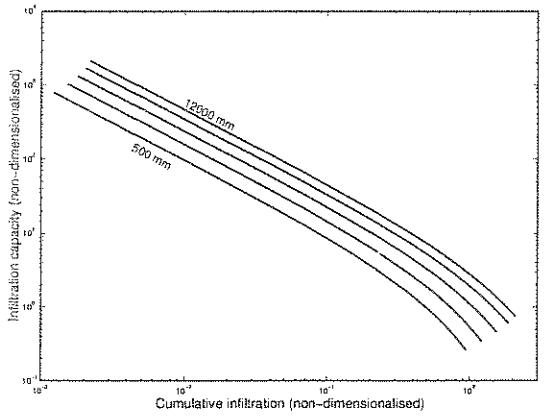

Figure 3. The relationship between $\overline{g^*}$ and $\overline{G}$ for different values of $\overline{D}$ ranging between 500 mm and 12000 mm.

A similar dependency test carried out for $\overline{K_s(0)}$ indicates an approximate invariance of the scaled $\overline{g^*}$ versus $\overline{G}$ relationship for a variety of storms. Thus we postulate an empirical equation for the intercept parameter a as

$$a = \overline{K_s(0)}(\alpha_1 + \beta_1 \overline{D}) \qquad (5)$$

where α_1 and β_1 are constants. Note that (5) could equally well have been expressed in terms of S_B rather than $\overline{D}$.

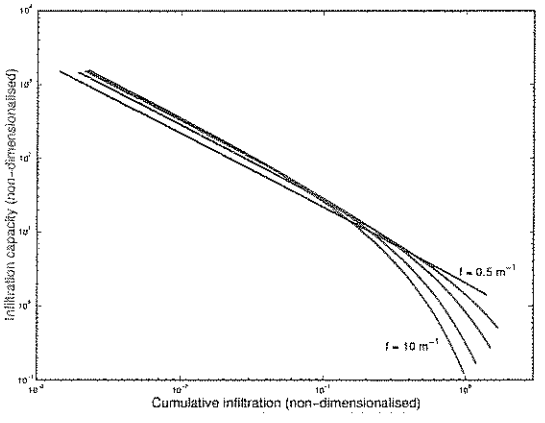

Figure 4. The relationship between $\overline{g^*}$ and $\overline{G}$ for different values of f ranging between 0.5 m^{-1} and 10 m^{-1}.

When the exponential decay parameter, f, is varied, with all other parameters remaining constant, the slope of the $\overline{g^*}$ versus $\overline{G}$ relationship increases with increasing values of f (Figure 4). Based on this systematic investigation, involving a large number of simulations, we assume a linear relationship between b and f, and can then postulate a functional form for the catchment scale infiltration capacity as

$$\overline{g^*} = \overline{K_s(0)}(\alpha_1 + \beta_1 \overline{D})\overline{G}^{-(\alpha_2+\beta_2 f)} \qquad (6)$$

We may now use (6) to predict the catchment-scale infiltration capacity, $\overline{g^*}$, as a function of the cumulative infiltration volume, $\overline{G}$, and the state of the permanent groundwater system (water table depth $\overline{D}$ or storage deficit S_B). Provided both the permanent groundwater deficit, S_B, and the state of an intermediate store representing the volume of infiltrated water are continuously updated, then on any given day, the infiltration capacity can be computed from (6). Given the volume of rainfall, $\overline{p}$, on this day, the infiltration-excess runoff generated will be the larger of $\{\overline{p} - \overline{g^*}, 0\}$ and the volume of actual infiltration will be the smaller of $\{\overline{p}, \overline{g^*}\}$. The volume of infiltrated water will then be used to update the intermediate infiltration store. The total runoff generated will be composed of both the infiltration-excess runoff calculated by (6) and the saturation-excess runoff given by (2).

It has to be noted that the simulations reported here have concentrated on only three parameters, namely $\overline{D}$, $\overline{K_s(0)}$ and f. This is because these are the parameters that have been shown to have the greatest impact on the volume of runoff generation [Sivapalan et al., 1987]. However, it is a trivial exercise to extend the simulations to help parameterise the remaining constants, α_1, α_2, β_1 and β_2 in (6) in terms of physically-based, measurable catchment attributes.

3. EVAPOTRANSPIRATION

The physics of evapotranspiration and plant water uptake at the point-scale is well-established. However, the large-scale hydrological modeller and the global climate modeller require parameterisations of evapotranspiration that integrate the point-scale responses over a large spatial domain. In general it is not feasible to apply point-scale equations directly to large areas because of the nonlinearity of the physically-based equations and the unknown spatial or vertical distributions of important environmental factors (e.g., root density, soil hydraulic properties), and because it is computationally impractical. Therefore we need some practical way to "scale up" the physically-based point-scale models to give catchment-scale parameterisations.

The large-scale evapotranspiration model described here was developed for the large-catchment hydrological model, LASCAM [Sivapalan et al., 1996], and will be developed with reference to the arrangement of stores pertaining to that model. However, it is envisaged that the technique will be equally suitable for other applications.

LASCAM models a catchment in terms of three inter-dependent conceptual soil water stores representing a near-stream, seasonal perched aquifer (the A store), the deep permanent groundwater system (B store) and an intermediate unsaturated infiltration zone (F store). The F store corresponds to the infiltration store G of the previous section, while the B store is an inverse of the storage deficit, S_B.

Evapotranspiration water may sourced from any of these three stores, provided there are roots present at suitable depths. It is assumed that, where the A store occurs in the landscape, evapotranspiration is drawn first from that store, since it is near the surface and represents a saturated source. Elsewhere in the landscape, or where the A store cannot satisfy demand, transpiration is drawn from the F store before it is drawn from the underlying B store. Consequently, we need an evaporation model that will allow us to partition the total evaporation among the three stores. Ideally, the resulting model should be as conceptually and mathematically simple as possible.

The physical models used for this analysis are based on those of Whisler et al. [1970] and Hoogland et al. [1981]. Water uptake depends on saturated hydraulic conductivity, root length and radius (distributed with depth), soil bubbling pressure, the Brooks and Corey parameter η, leaf area, potential evaporation, and the distribution of soil water potential with depth.

In building the model we assume that the catchment can be collapsed into a single, two-dimensional hillslope with simple idealised geometry. We then assume random, but realistic, values of the input variables (i.e, those controlling water uptake and those describing the hillslope and watertable geometry) in the physically-based point-scale model. The notional soil moisture at all points on the hillslope is distributed according to the levels of the three soil water stores. Here we assume that the A and B stores are saturated and that in the F store, moisture content increases with store volume.

The point-scale model is applied at a large number of regularly-spaced points on the hillslope, and the evaporation responses are integrated to yield catchment-scale extractions from each store. We repeat this procedure for different values of the store levels and of the physical variables.

The model simulations based on the simple hillslope geometry confirm that the evaporation rate from the A store may be determined analytically in terms of leaf area and a geometric parameter that depends on catchment slope and A horizon depth. As such, it is not reliant on the disaggregation-aggregation approach, and will not be discussed here.

The generalised evapotranspiration responses from the B and F stores could not be derived analytically. The F store evaporation curve typically takes the sigmoidal shape shown in Figure 5. Although this response curve could have been modelled better by a more complicated function (e.g., a cubic), we chose for simplicity to model only the upper part of the curve (above the inflection point), as it too, appears linear on a log-log graph. This suggests a catchment-scale relationship of the form

$$e_F = \alpha_F e_p L (1 - F/F_{max})^{\beta_F} \qquad (7)$$

where F is the level of the F store, F_{max} is a F store scaling factor, e_p is the potential evaporation remaining after evaporation has been extracted from the A store, L is the leaf area index, and α_F and β_F are optimisable parameters that incorporate the effects of root distribution and soil properties. Equation 7 thus neglects that amount of F store evaporation that is associated with small values of F, but the effect of this underprediction is small. Examples of the F store evaporation response for ten representative sets of input variables, together with the fitted catchment-scale model are shown in Figure 5.

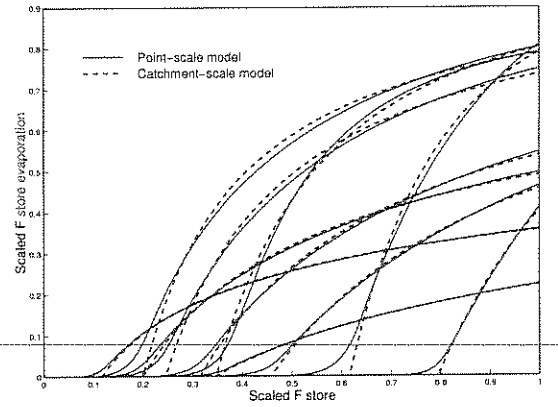

Figure 5. Relationship between the F store volume (scaled by F_{max}) and its evaporation response (scaled by Le_p) for the aggregated point-scale model and for the catchment-scale model given by (7).

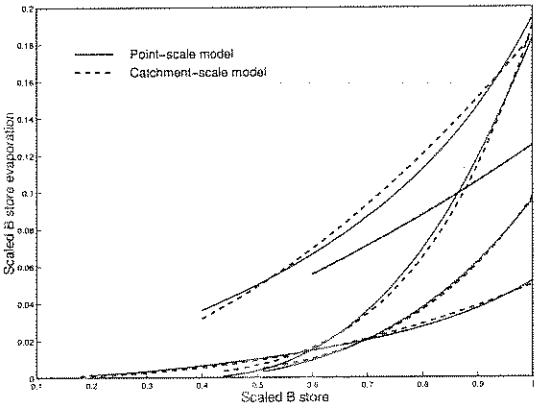

Figure 6. Relationship between the B store (scaled by B_{max}) and its evaporation response (scaled by Le_p) for the aggregated point-scale model and for the catchment-scale model given by (8).

The B store evaporation curve typically takes an exponential shape, but may be approximated by a straight line on a log-log graph. This suggests that the response can be described by

$$e_B = \alpha_B e_p L(B/B_{max})^{\beta_B} \quad (8)$$

where B is the level of the B store, B_{max} is a B store scaling factor and α_B and β_B are optimisable parameters. Here, e_p is the potential evaporation remaining after any evaporation has been removed from the A and F stores. Examples of this B store evaporation response for five representative sets of input variables, together with the fitted catchment-scale model are shown in Figure 6.

4. CONCLUSIONS

This paper has described a methodology to develop catchment-scale conceptualisations by integrating point-scale, process-based descriptions. A key aspect has been the ability to link the state variables representing the antecedent soil moisture state of the catchment between the catchment and local scales. This approach was illustrated by two examples in which catchment-scale models of infiltration-excess runoff and evapotranspiration were developed. In the former case, the methodology involved both the temporal disaggregation of daily inputs and the spatial disaggregation of the state variables (moisture content). In both cases, spatial disaggregation took advantage of the natural organisation of moisture content within a catchment.

All conceptual rainfall runoff models necessarily have at least one component that models the volume of runoff generation and most also include models of evapotranspiration. These models are typically expressed in terms of the status of one or more conceptual stores. In the past the functional forms of these constitutive relations were often assumed arbitrarily and their parameters estimated by calibration. Typically, the physical bases of these functions have not been investigated. This paper represents an attempt to develop such links between the conceptual model parameterisations and the underlying process-based, small-scale descriptions. In the case of the infiltration model (and potentially for the evapotranspiration model), the sensitivity analyses have given considerable insights into the physical meaning of the lumped model parameters. As a result, the measurability of the catchment-scale parameterisations has been substantially enhanced.

It is important to emphasise that the disaggregation-aggregation approach scales model output, rather than actual catchment behaviour. The resulting catchment-scale conceptualisations are only reliable and effective in so far as the point formulations they are derived from do indeed represent reality and encompass all the factors that have a significant influence on hydrological variability.

The relations developed in this paper are intended for use in lumped catchment models operating at a daily time step. They have been integral to the development of the LASCAM model [Sivapalan et al., 1996]. The disaggregation-aggregation approach outlined here has been used to conceptualise many of the hydrological fluxes in LASCAM (e.g., subsurface stormflow) and has potential application in the development of other conceptual hydrological models.

5. ACKNOWLEDGEMENTS

The authors are indebted to Charles Jeevaraj and Jens Larsen for their assistance in developing the infiltration and evapotranspiration models.

6. REFERENCES

Beven, K.J., and M.J. Kirkby, A physically-based variable contributing area model of basin hydrology, *Hydrological Science Bulletin, 24*, 43–69, 1979.

Brooks, R.H., and A.T. Corey, Hydraulic properties of porous media, Hydrology Papers 3, Colorado State University, Fort Collins, United States, 27pp., 1964.

Green, W.H., and G.A. Ampt, Studies on soil physics, Part I. The flow of air and water through soils, *Journal of Agricultural Science, 4*, 1–24, 1911.

Hoogland, J.C., R.A. Feddes and C. Belmans, Root water uptake model depending on soil water pressure head and maximum extraction rate, *Acta Horticulturae, 119*, 123–135, 1981.

Sivapalan, M., Linking hydrologic parameterizations across a range of spatial scales: hillslope to catchment to region, IAHS Publication Number 212, Proceedings of Yokohama Symposium, 115–123, 1993.

Sivapalan, M., J.K. Ruprecht and N.R. Viney, Water and salt balance modelling to predict the effects of land use changes in forested catchments. 1. Small catchment water balance model, *Hydrological Processes, 10*, 393–411, 1996.

Sivapalan, M., K. Beven and E.F. Wood, On hydrologic similarity. 2. A scaled model of storm runoff production, *Water Resources Research, 23*, 2266–2278, 1987.

Sivapalan, M., E.F. Wood and K.Beven, On hydrologic similarity. 3. A dimensionless flood frequency model using a generalized geomorphologic unit hydrograph and partial area runoff generation, *Water Resources Research, 26*, 43–58, 1990.

Whisler, F.D., A. Klute and R.J. Millington, Analysis of radial, steady-state solution, and solute flow, *Soil Science Society of America Proceedings, 34*, 382–387, 1970.